Phonon-Photon Mapping in a Color Center in Hexagonal Boron Nitride

T. Q. P. Vuong,[1] G. Cassabois,[1] P. Valvin,[1] A. Ouerghi,[2] Y. Chassagneux,[3] C. Voisin,[3] and B. Gil[1,*]
[1]Laboratoire Charles Coulomb, UMR 5221 CNRS-Université de Montpellier, 34095 Montpellier, France
[2]Laboratoire de Photonique et de Nanostructures (CNRS-LPN), Route de Nozay, 91460 Marcoussis, France
[3]Laboratoire Pierre Aigrain, Ecole Normale Supérieure, Université Paris Diderot, UPMC, CNRS UMR8551, 24 rue Lhomond, 75005 Paris, France
(Received 23 March 2016; published 25 August 2016)

We report on the ultraviolet optical response of a color center in hexagonal boron nitride. We demonstrate a mapping between the vibronic spectrum of the color center and the phonon dispersion in hexagonal boron nitride, with a striking suppression of the phonon assisted emission signal at the energy of the phonon gap. By means of nonperturbative calculations of the electron-phonon interaction in a strongly anisotropic phonon dispersion, we reach a quantitative interpretation of the acoustic phonon sidebands from cryogenic temperatures up to room temperature. Our analysis provides an original method for estimating the spatial extension of the electronic wave function in a point defect.

DOI: 10.1103/PhysRevLett.117.097402

Hybrid quantum systems aim at combining the electronic, vibronic, and photonic degrees of freedom into tripartite excitations [1]. This novel field emerges at the intersection of cavity quantum electrodynamics [2] and optomechanics [3], with impressive recent developments such as the integration of superconducting qubits with micromechanical resonators [4], or the coupling of propagating phonons with an artificial atom [5].

In this context, the rising interest in two-dimensional (2D) atomic crystals and their van der Waals heterostructures [6] has resulted in various experiments paving the way for the implementation of hybrid quantum systems in 2D materials. The strong coupling regime of the electronic-photonic interaction has been achieved by embedding transition metal dichalcogenide monolayers in an optical microcavity, enabling the observation of exciton polaritons [7,8]. The vibronic-photonic coupling has been explored in graphene, and the use of graphene membranes as a mechanical resonator has allowed the demonstration of its optomechanical coupling with a microwave cavity [9]. Although the propagation of surface acoustic waves was evidenced in graphene for acoustoelectronics applications [10], there is however no work on the electronic-vibronic interaction in artificial atoms in 2D crystals, and more generally in layered materials, but only the report of quantum light emission in localized states in WSe_2 [11–13] and hexagonal boron nitride (hBN) [14].

In this Letter, we report on the ultraviolet (UV) optical response of a color center in hBN. In the emission spectrum, we resolve a narrow zero-phonon line and phonon sidebands, which remarkably map the bulk phonon dispersion in hBN. We show that the vibronic spectrum reflects the density of states of bulk phonons in hBN, with a striking suppression of the phonon assisted emission signal at the energy of the hBN phonon gap. Moreover, we do not observe any signature related to local vibration modes, contrarily to other color centers in semiconductors, such as the prototype nitrogen vacancy center in diamond [15]. By means of nonperturbative calculations of the electron-phonon interaction in a point defect, we reach a quantitative interpretation of the sidebands due to the long-wavelength bulk acoustic phonons, which are at the basis of sideband cooling protocols [16] or coherent phonon manipulation [5,17]. From this analysis, we also obtain the first estimation of the deformation potential in hBN, together with the characteristic spatial extension of the defect of 2 ± 0.3 Å.

hBN is a wide-band-gap nitride semiconductor with a lamellar crystalline structure analog to graphite [18]. Its fundamental band gap is indirect with a dim excitonic emission at 5.955 eV [19], and intense phonon replicas between 5.7 and 5.9 eV, as seen in Fig. 1. In our measurements, a commercial hBN crystal from HQ Graphene is held on the cold finger of a closed-cycle cryostat, and after nonresonant excitation at 6.3 eV by the fourth harmonic of a Ti:sapphire oscillator, the photoluminescence (PL) signal is detected by an achromatic optical system [20]. The presence of defects in hBN leads to two additional emission bands centered at 5.5 and 4 eV [21–26]. The former comes from extended defects or stacking faults (red shaded area in Fig. 1), which were in particular characterized with a nanometric resolution in a transmission electron microscope [27]. It was also recently demonstrated that most of the lines observed in the broad emission spectrum between 4.8 and 5.7 eV consist in resonances of the phonon assisted carrier relaxation rate, with an energy spacing reflecting intervalley scattering [20].

Below 4.8 eV, the emission spectrum in bulk hBN displays a band related to deep levels (green shaded area in Fig. 1), corresponding to electronic states localized in point defects [21,22,25,28]. Moreover, we observe substructures, and in particular a sharp peak at 4.1 eV, a weaker one at 3.9 eV, and a third one at 3.7 eV barely observable

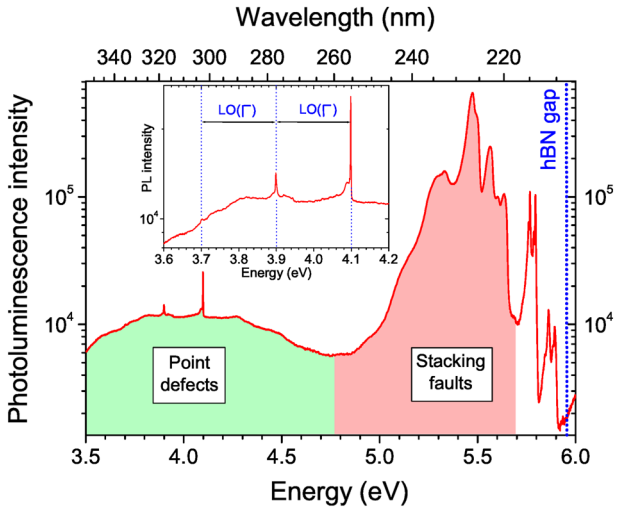

FIG. 1. Photoluminescence spectrum in bulk hBN at 10 K (solid red line) on a 2.5-eV energy range, for an excitation at 6.3 eV. The vertical dotted blue line indicates the hBN band gap at 5.95 eV. The green (red) shaded area corresponds to the emission of point defects (stacking faults). Inset: enlargement around 3.9 eV.

atop the broad emission background, as shown in the inset of Fig. 1 displaying an enlargement around 3.9 eV. In contrast to previous studies focusing on this multiplet of peaks in hBN and concluding to the existence of phonon replicas in a point defect [22,25,28], we resolve here the complete vibronic spectrum by means of high-spectral resolution in PL experiments in hBN single crystals at 10 K. We first demonstrate the presence of a previously unresolved zero-phonon line (ZPL) in the emission spectrum, lying at 4.1 eV with a full width at half maximum (FWHM) as narrow as 2 meV (Fig. 1). Such a value is of the order of the linewidth measured in single quantum dots in state-of-the-art AlGaN-based samples for single photon sources in the UV range [29,30]. The fact that we observe similar values by means of ensemble measurements is a strong indication for the well-defined, excellent structural properties of this UV color center. However, in Fig. 1 the PL signal of the color center appears to be superimposed on the broad emission background, approximately at its maximum intensity, making difficult a further investigation of the color center optical properties, at least in this configuration where we perform above band gap excitation at 6.3 eV.

We thus switch to below band gap excitation in order to suppress the 4-eV broad emission background, following the excitation spectroscopy measurements performed below 4.75 eV and reported in Ref. [25]. In Fig. 2, we display, on a semilog scale, the PL signal intensity (solid red line) as a function of the energy detuning with the 4.1-eV energy of the ZPL. In this background-free configuration, we observe that the vibronic spectrum does not only consist in a low-energy sideband with a maximum intensity for a 10 meV redshift, and that secondary maxima are observable at −40 and −70 meV energy detunings. Moreover, the PL signal intensity decreases to the noise level for a detuning of −145 meV, which coincides with the phonon gap in hBN [31,32]. For larger detunings, the PL signal intensity increases with a steep rise to a relative maximum at −155 meV, followed by a broader line until −180 meV, and finally a sharp asymmetric line at −200 meV, i.e., the absolute maximum of the optical phonon energy in hBN, corresponding to zone-center longitudinal optical [LO(Γ)] phonons.

In light of the vibronic spectrum inspection correlating with specific energies of the phonon band structure in hBN, we further compare the PL spectrum of our UV color center with the phonon density of states in hBN [31] (blue dotted line in Fig. 2). We first observe that the peaks at −40, −70, −155, and −180 meV all correspond to extrema of the phonon density of states in different high-symmetry points of the Brillouin zone, and related to ZA(K), ZO(K), TO(M)/LO(K), and LO(T) phonons, respectively. In the case of zone-edge phonons, the electron-phonon interaction via the deformation potential is known to be weakly dependent on the phonon wave vector k [33], whereas at the zone center, the deformation potential and the piezoelectric coupling scale like $\sqrt{k}$ and $1/\sqrt{k}$, respectively, while the Fröhlich interaction varies like $1/k$. Such a weak k dependence of the deformation potential at the zone edge is well documented in the context of intervalley scattering in indirect and direct band gap semiconductors [34–36]. As a matter of fact, the efficiency of the corresponding phonon assisted

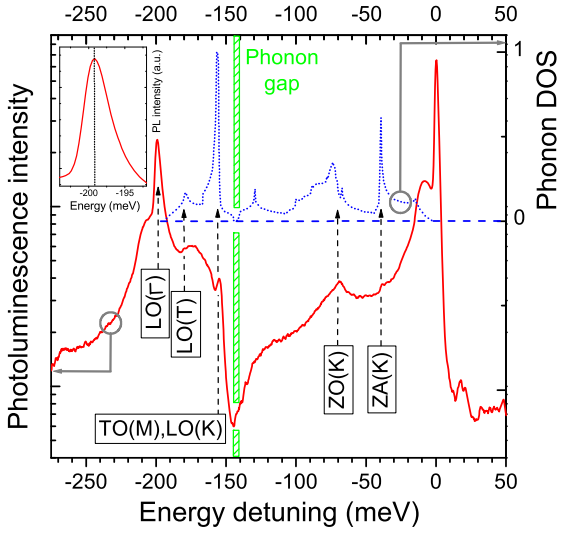

FIG. 2. Photoluminescence signal intensity at 10 K (solid red line), on a semilog scale, for an excitation at 4.6 eV, as a function of the energy detuning with the zero-phonon line of the color center emitting at 4.1 eV (Fig. 1), compared to the phonon density of states in hBN (blue dotted line) from Ref. [31]. Inset: enlargement of the PL spectrum around −200 meV.

recombination will mainly reflect the phonon density of states, provided that first-order processes involving only one phonon are dominant in the optical response. The one-by-one identification of the phonon sideband peaks with the extrema of the phonon density of states (Fig. 2) indicates that we are, at low temperature, in the regime where one-phonon scattering processes dominate. This interpretation is further supported by the striking observation of a pronounced dip in the vibronic spectrum (down to our noise level) exactly in the 5 meV spectral range of the phonon gap in hBN (green dashed area in Fig. 2). To the best of our knowledge, it is the first evidence of such a suppression of the phonon sideband in the spectral region of a phonon gap, in point defects and more generally in semiconductor nanostructures.

In contrast to phonons at the boundaries of the Brillouin zone, zone-center phonons couple to electrons through strongly k dependent interactions [33]. In the case of optical phonons, the Fröhlich interaction scales like the inverse of the phonon wave vector, resulting in a divergence of the electron-phonon matrix element for zone-center longitudinal optical phonons. This singularity accounts for the intense phonon sideband at −200 meV (Fig. 2), despite the vanishing density of states at the energy of the LO(Γ) phonons in hBN. Interestingly, the usual negative curvature of the LO phonon branch around Γ is expected to result in a tail of the LO(Γ) sideband towards smaller energy detunings, which has never been observed so far. The asymmetric line profile around −200 meV in Fig. 2 (inset) provides a textbook example for this effect.

As far as zone-center acoustic phonons are concerned, we present below a quantitative interpretation of the low-energy vibronic spectrum, which will allow us to extract estimations of the defect size and deformation potential, and to reproduce the temperature-dependent measurements up to room temperature, displayed in Fig. 3. Phonon assisted optical processes in point defects were described in the early years of solid-state physics, in particular in the pioneering study of Huang and Rhys [37]. In this paper, the authors analyzed the optical absorption of F centres on the basis of the Franck-Condon principle. A description to all orders in the electron-phonon interaction was later developed by Duke and Mahan within a Green function formalism [38], with a renewed interest in the context of semiconductor quantum dots and nanocrystals. In order to interpret time-resolved experiments of the coherent nonlinear response in semiconductor quantum dots, Krummheuer *et al.* calculated the time-dependent polarization after pulsed excitation, and they derived an analytical expression of the nonperturbative optical response for the coupling to phonons [39]. Such a nonperturbative approach takes into account the coupling terms to all orders in the exciton-phonon interaction, thus accounting for the radiative recombination assisted by the emission of any phonon number. This aspect is particularly important

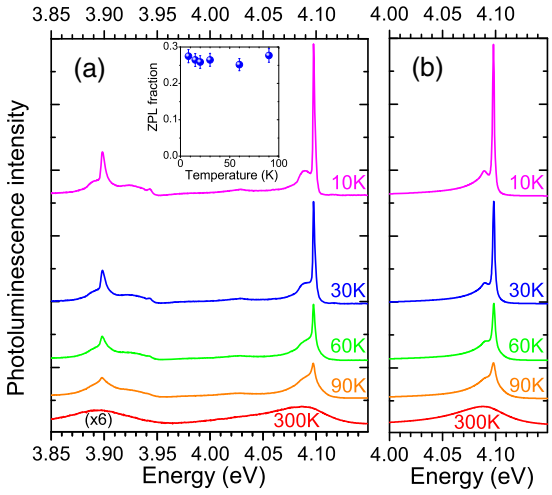

FIG. 3. (a) Photoluminescence spectrum of the 4.1-eV color center in hBN, for an excitation at 4.6 eV, from 10 to 300 K. Inset: fraction of the emission in the ZPL as a function of temperature. (b) Calculations of the longitudinal acoustic phonon sidebands, from 10 to 300 K, with a deformation potential $D = 11$ eV and a point defect extension $\sigma = 2$ Å.

on increasing the temperature where the phonon sidebands are no longer limited to the one-phonon processes, which usually dominate at low temperature [39,40], so that a nonperturbative approach becomes mandatory at high temperature.

In the framework of this theoretical approach, we have calculated the emission spectrum of the 4.1-eV color center in hBN in order to quantitatively account for our PL measurements (Fig. 3). More specifically, we have computed the sidebands arising from the coupling to acoustic phonons. Close to the zone center, the deformation potential interaction is allowed only for longitudinal acoustic (LA) phonons, while piezoelectric coupling is allowed for both LA and TA phonons [39]. hBN being centrosymmetric and thus nonpiezoelectric, the only remaining coupling is the deformation potential for LA phonons. The emission spectrum is thus obtained by taking the Fourier transform of the time-dependent linear susceptibility $\chi(t)$ given by [39]

$$\chi(t) = \exp\left[\sum_{\mathbf{k}} |\gamma_{\mathbf{k}}|^2 (e^{-i\omega(\mathbf{k})t} - n(\mathbf{k})|e^{-i\omega(\mathbf{k})t} - 1|^2 - 1)\right], \quad (1)$$

where $\omega(\mathbf{k})$ is the energy of a LA phonon of wave vector $\mathbf{k}$, $n(\mathbf{k})$ is the corresponding Bose-Einstein phonon occupation factor, and $\gamma_{\mathbf{k}}$ is a dimensionless coupling strength (see Ref. [41] for more details on the model). Importantly, we have taken into account the anisotropic sound dispersion in hBN resulting from the peculiar crystalline properties of this lamellar compound, so that

$\omega(\mathbf{k})$ reads $\sqrt{(c_{s,\|}k_\|)^2 + (c_{s,z}k_z)^2}$, where $\mathbf{k}_\|$ ($c_{s,\|}$) and k_z ($c_{s,z}$) are the in-plane and out-of-plane wave vectors (sound velocities), with the Oz direction along the c axis of hBN, and $c_{s,\|}/c_{s,z} \sim 7.5$ [32].

In our calculations, we have three free parameters: the magnitude D of the deformation potential, the extension σ of the electronic wave function in the color center, and the FWHM of the ZPL labeled Γ_{ZPL}. Γ_{ZPL} is a phenomenological broadening introduced in the model, since the latter does not account for the thermally assisted broadening of the ZPL [39]. Its value is adjusted for each temperature in order to reproduce the ZPL (see Ref. [41] for more details on the ZPL broadening). In Fig. 3, we display the comparison between our temperature-dependent measurements from 10 to 300 K [Fig. 3(a)] and our calculations of the longitudinal acoustic phonon sidebands [Fig. 3(b)] for fixed values of the deformation potential ($D = 11$ eV) and point defect extension ($\sigma = 2$ Å). We observe an excellent agreement for the complete set of data. In particular, we fully account for the smooth transition to a symmetric emission spectrum on raising the temperature. While phonon emission gives rise to a redshifted emission after phonon assisted recombination, phonon absorption leads on the contrary to a blueshifted emission with respect to the ZPL. At low temperature, the probability of phonon absorption is negligible compared to phonon emission, leading to an asymmetric vibronic spectrum (Fig. 3, 10 K). When raising the temperature, phonon absorption becomes more and more probable, resulting in a high-energy sideband of growing intensity (Fig. 3, 30–90 K), up to a quasisymmetric emission spectrum at room temperature (Fig. 3, 300 K). Furthermore, we note that the visibility of the ZPL decreases as a function of temperature. Nevertheless, as long as it is observable, i.e., below 100 K, the fraction of the emission in the ZPL, often called the Debye-Waller factor, remains constant [Fig. 3(a), inset]. The decreasing visibility of the ZPL arises in fact from its broadening, which reduces the maximum intensity of the ZPL on top of the Γ_{ZPL}-independent vibronic spectrum [41]. Eventually, we highlight that the longitudinal acoustic phonon sidebands involve both in-plane and out-of-plane phonons, in contradiction to early studies on the electron-phonon interaction in a layered compound tentatively predicting the implication of only rigid-layer modes with a k_z wave vector [43]. In Eq. (1), the truncated sum to only $\{k_z\}$ wave vectors does lead to a drastic reduction of the sideband intensity, infirming the hypothesis of Ref. [43] and thus showing the combined action of in-plane and out-of-plane phonons in the sideband buildup.

In our model, the free intrinsic parameters are the defect extension σ and the deformation potential D. Although the latter can *a priori* be estimated from independent experiments [33] and is usually tabulated for a number of semiconductor compounds, the only recent synthesis of high-quality hBN crystals makes the literature completely nonexistent on this topic. Nevertheless, the observation of the sideband maximum at an energy detuning of -10 meV in our low temperature measurements turns out to be decisive for reaching an accurate estimation of both fitting parameters. When varying the values of D and σ, the sideband maximum changes in energy and in intensity [41], the latter being directly related to the Debye-Waller factor. In order to reproduce both the energy and the intensity of the sideband maximum at 10 K, we have to take $D = 11 \pm 0.5$ eV and $\sigma = 2 \pm 0.3$ Å. The 11-eV value of the deformation potential has to be compared with the absolute value of the difference $D_e - D_h$ between the deformation potentials D_e and D_h for electrons and holes, respectively [41]. From the theoretical estimations in the literature [44–46], we deduce that $|D_e - D_h|$ ranges from 1.7 to 8 eV. However, these calculations performed within the density functional theory without *GW* corrections underestimate the band gap of hBN by 30%, and therefore possibly also the deformation potentials, so that corrected theoretical estimations will have higher values with an upper bound close to our estimate. As far as the extension of the electronic wave function is concerned, the 2-Å value is of the order of the in-plane B–N bond length (1.4 Å), but smaller than the interlayer distance in hBN (3.3 Å), suggesting a ponctual alteration of the in-plane crystalline structure. The 2-Å extension of the color center also corroborates the observation of zone-edge phonon replicas in the PL spectrum (Fig. 2), requiring a defect extension comparable to the inverse of the phonon wave vector in the form factor describing the electron-phonon coupling efficiency [39]. These results should stimulate further investigation by local probe techniques in order to achieve the chemical identification of this defect center. It might be a nitrogen vacancy V_N bound to a carbon or an oxygen atom [28], although Stone-Wales defects transforming two hexagons into a pentagon and a heptagon could also form preferential sites for adsorbates.

In summary, we have studied the vibronic spectrum in a color center in hexagonal boron nitride. We have shown that the vibronic spectrum reflects the density of states of bulk phonons in hexagonal boron nitride, with a striking suppression of the phonon assisted emission signal at the energy of the phonon gap. By means of nonperturbative calculations of the electron-phonon interaction in a strongly anisotropic phonon dispersion, we reach a quantitative interpretation of the acoustic phonon sidebands from cryogenic temperatures up to room temperature, allowing us to estimate the deformation potential value and the spatial extension of the defect. These unique features of the electronic-vibronic interaction in this color center are supplemented by the recent success in isolating such a single color center, which displays bright single photon emission in antibunching experiments [47]. These results pave the way for the implementation of hybrid quantum

systems in layered materials, using this color center as a fundamental building block.

We gratefully acknowledge C. L'Henoret for his technical support at the mechanics workshop, and V. Jacques, L. Tizei, M. Kociak, and A. Zobelli for fruitful discussions. This work was financially supported by the network GaNeX (ANR-11-LABX-0014). GaNeX belongs to the publicly funded *Investissements d'Avenir* program managed by the French ANR agency.

*bernard.gil@umontpellier.fr

[1] J. Restrepo, C. Ciuti, and I. Favero, Phys. Rev. Lett. **112**, 013601 (2014).
[2] S. Haroche and J. M. Raimond, *Exploring the Quantum*, Oxford Graduate Texts (Oxford, New York, 2006).
[3] F. Marquardt and S. M. Girvin, Physics **2**, 40 (2009).
[4] J. M. Pirkkalainen, S. U. Cho, J. Li, G. S. Paraoanu, P. J. Hakonen, and M. A. Sillanpää, Nature (London) **494**, 211 (2013).
[5] M. V. Gustafsson, T. Aref, A. F. Kockum, M. K. Ekström, G. Johansson, and P. Delsing, Science **346**, 207 (2014).
[6] A. K. Geim and I. V. Grigorieva, Nature (London) **499**, 419 (2013).
[7] X. Liu , T. Galfsky, Z. Sun, F. Xia, E.-c. Lin, Y.-H. Lee, S. Kéna-Cohen, and V. M. Menon*et al.*, Nat. Photonics **9**, 30 (2015).
[8] S. Dufferwiel *et al.*, Nat. Commun. **6**, 8579 (2015).
[9] V. Singh, S. J. Bosman, B. H. Schneider, Y. M. Blanter, A. Castellanos-Gomez, and G. A. Steele, Nat. Nanotechnol. **9**, 820 (2014).
[10] V. Miseikis, J. E. Cunningham, K. Saeed, R. ORorke, and A. G. Davies, Appl. Phys. Lett. **100**, 133105 (2012).
[11] A. Srivastava, M. Sidler, A. V. Allain, D. S. Lembke, A. Kis, and A. Imamoğlu, Nat. Nanotechnol. **10**, 491 (2015).
[12] Y. M. He *et al.*, Nat. Nanotechnol. **10**, 497 (2015).
[13] M. Koperski, K. Nogajewski, A. Arora, V. Cherkez, P. Mallet, J.-Y. Veuillen, J. Marcus, P. Kossacki, and M. Potemski, Nat. Nanotechnol. **10**, 503 (2015).
[14] T. T. Tran, K. Bray, M. J. Ford, M. Toth, and I. Aharonovich, Nat. Nanotechnol. **11**, 37 (2016).
[15] A. Alkauskas, B. B. Buckley, D. D. Awschalom, and C. G. Van de Walle, New J. Phys. **16**, 073026 (2014).
[16] I. Wilson-Rae, P. Zoller, and A. Imamoglu, Phys. Rev. Lett. **92**, 075507 (2004).
[17] A. Albrecht, A. Retzker, F. Jelezko, and M. B. Plenio, New J. Phys. **15**, 083014 (2013).
[18] K. Watanabe, T. Taniguchi, and H. Kanda, Nat. Mater. **3**, 404 (2004).
[19] G. Cassabois, P. Valvin, and B. Gil, Nat. Photonics **10**, 262 (2016).
[20] G. Cassabois, P. Valvin, and B. Gil, Phys. Rev. B **93**, 035207 (2016).
[21] A. Katzir, J. T. Suss, A. Zunger, and A. Halperin, Phys. Rev. B **11**, 2370 (1975).
[22] M. G. Silly, P. Jaffrennou, J. Barjon, J.-S. Lauret, F. Ducastelle, A. Loiseau, E. Obraztsova, B. Attal-Trétout, and E. Rosencher, Phys. Rev. B **75**, 085205 (2007).
[23] P. Jaffrennou, J. Barjon, J.-S. Lauret, B. Attal-Trétout, F. Ducastelle, and A. Loiseau, J. Appl. Phys. **102**, 116102 (2007).
[24] L. Museur and A. Kanaev, J. Appl. Phys. **103**, 103520 (2008).
[25] L. Museur, E. Feldbach, and A. Kanaev, Phys. Rev. B **78**, 155204 (2008).
[26] K. Watanabe and T. Taniguchi, Int. J. Appl. Ceram. Technol. **8**, 977 (2011).
[27] R. Bourrellier *et al.*, ACS Photonics **1**, 857 (2014).
[28] X. Z. Du, J. Li, J. Y. Lin, and H. X. Jiang, Appl. Phys. Lett. **106**, 021110 (2015).
[29] M. J. Holmes, K. Choi, S. Kako, M. Arita, and Y. Arakawa, Nano Lett. **14**, 982 (2014).
[30] G. Hönig, G. Callsen, A. Schliwa, S. Kalinowski, C. Kindel, S. Kako, Y. Arakawa, D. Bimberg, and A. Hoffmann, Nat. Commun. **5**, 5721 (2014).
[31] G. Kern, G. Kresse, and J. Hafner, Phys. Rev. B **59**, 8551 (1999).
[32] J. Serrano, A. Bosak, R. Arenal, M. Krisch, K. Watanabe, T. Taniguchi, H. Kanda, A. Rubio, and L. Wirtz, Phys. Rev. Lett. **98**, 095503 (2007).
[33] In *Fundamentals of Semiconductors*, edited by P. Y. Yu and M. Cardona (Springe-Verlag, Berlin Heidelberg, 1996).
[34] S. Zollner, S. Gopalan, and M. Cardona, Appl. Phys. Lett. **54**, 614 (1989).
[35] S. Zollner, S. Gopalan, and M. Cardona, J. Appl. Phys. **68**, 1682 (1990).
[36] S. Gopalan, P. Lautenschlager, and M. Cardona, Phys. Rev. B **35**, 5577 (1987).
[37] K. Huang and A. Rhys, Proc. R. Soc. A **204**, 406 (1950).
[38] C. B. Duke and G. D. Mahan, Phys. Rev. **139**, A1965 (1965).
[39] B. Krummheuer, V. M. Axt, and T. Kuhn, Phys. Rev. B **65**, 195313 (2002).
[40] L. Besombes, K. Kheng, L. Marsal, and H. Mariette, Phys. Rev. B **63**, 155307 (2001).
[41] See Supplemental Material at http://link.aps.org/supplemental/10.1103/PhysRevLett.117.097402, for more information on the calculations of the phonon-assisted recombination line, the broadening of the zero-phonon line, and the determination of the deformation potential and defect extension, which includes Refs. [39,42].
[42] I. Favero, G. Cassabois, R. Ferreira, D. Darson, C. Voisin, J. Tignon, C. Delalande, G. Bastard, Ph. Roussignol, and J. M. Gérard, Phys. Rev. B **68**, 233301 (2003).
[43] T. Kuzuba, K. Era, T. Ishii, T. Sato, and M. Iwata, Physica A (Amsterdam) **105B**, 339 (1981).
[44] S. Bruzzone and G. Fiori, Appl. Phys. Lett. **99**, 222108 (2011).
[45] J.-T. Sun, A. T. S. Wee, and Y. P. Feng, AIP Adv. **2**, 032133 (2012).
[46] A. Bhattacharya, S. Bhattacharya, and G. P. Das, arXiv:1101.5245.
[47] R. Bourrellier, S. Meuret, A. Tararan, O. Stéphan, M. Kociak, L. H. G. Tizei, and A. Zobelli, Nano Lett. **16**, 4317 (2016).